

# A Study for the Influence of Work Hardening on Bending Stiffness of Truss Core Panel

**Sunao Tokura**

Engineering Division,  
JSOL,  
2-5-24, Harumi,  
Chuo-ku, Tokyo 104-0053, Japan  
e-mail: tokura.sunao@jsol.co.jp

**Ichiro Hagiwara**

Department of Mechanical Sciences and  
Engineering and Graduate School of Science and  
Engineering,  
Tokyo Institute of Technology,  
2-21-1, O-okayama,  
Meguro-ku, Tokyo 152-8552, Japan

*Honeycomb panel is widely used as flooring or wall material in various structures, e.g., buildings, aircraft, flooring members of railway car, and so on, due to high stiffness and lightness at present. Honeycomb panel, however, has a disadvantage that the adhesive used to glue honeycomb core and top plate may burn by fire. On the other hand, truss core panel has equivalent stiffness as honeycomb panel and is expected to be an alternative to honeycomb panel as it is safer for fire. To replace honeycomb panel with truss core panel, it is necessary to investigate the stiffness of truss core panel for bending, shear, compression, and so on. The bending case with a three-point bending model of truss core panel is chosen here. Four cases of analysis with/without work hardening effect and thickness change using two types of shell formulation are performed. These cases are compared with an equivalent honeycomb model. The study showed the effect of work hardening is very important to assess bending stiffness of truss core panel. It is also observed that the use of suitable shell formulation is necessary to obtain reliable result. In addition, the truss core panel shows bending stiffness comparable with conventional honeycomb panel. [DOI: 10.1115/1.4000419]*

**Keywords:** origami-engineering, truss core panel, multistage forming simulation, press working, finite element method, bending stiffness, work hardening, shell formulation, full integration shell, reduced integration shell

## 1 Introduction

Honeycomb panel glued honeycomb core with surface plates has widely been used for buildings, aircrafts, flooring members of railway car, and so on as lightweight structure with high strength. Honeycomb panels can be manufactured rather easily for many kinds of core and panel sizes as usage and have the feature of high bending stiffness as structural member. They, however, have rather frugal strength against shear deformation and in-plane compressive load. A risk for the panel is pointed out that the adhesive being used to glue honeycomb core and surface plates may be burned as a fire happens. Consequently, from the prospect of application to origami-engineering, truss core panels [1,2] have been focused because the panels can be manufactured of only metal as alternative for honeycomb panel. The truss core panel is a structural material invented from the study on the theory of space filling using regular tetrahedron and octahedron. As many kinds of usage for the truss core panel can be considered as alternatives of honeycomb one, a feature for its strength is needed to examine [3].

The truss core itself will be formed from many kinds of materials such as plastics and so on. However, thin metal plates will be used generally in the case that the truss core panel is employed as structural member. And yet in case of checking its strength as structural member, some loading modes have to be assumed, e.g., out-of-plane bending loading, out-of-plane/in-plane shears loading, and so on. So the authors focus on the bending stiffness first and try to check the bending behavior of truss core panel with simulation using nonlinear finite element method (FEM). In the case that truss core panel is employed as practical, structural member, two cases are considered: one is single truss core panel only or two panels are welded for strengthening. In the latter, one

panel of two is turned upside down and the vertices of the cores on the plate and the flat surface of the other are spotwelded all together.

As an actual truss core panel is formed from a flat metal sheet by plastic forming such as press forming and so on, the effect of plastic forming have to be considered for the estimation of stiffness after the truss core panel is formed. The authors have proposed the multistage press forming process of steel truss core panel before [4]. Using the results obtained from the press forming simulation with FEM performed at the time, the stiffness was estimated considering work hardening. The bending stiffness of the truss core panel was compared with the one of honeycomb panel through FE simulation.

In addition the influence of shell element formulation to the result of structure, an analysis using nonlinear finite element method was also investigated. In this study explicit FEM, which is suitable for large-scale nonlinear numerical simulation, is applied and a commercial explicit FEM software LS-DYNA [5] was adopted for this purpose.

## 2 Creation of the Analysis Model

**2.1 Basic Geometry of the Truss Core Panel.** Figure 1 shows the geometry and dimensions of the truss core panel to be targeted in this paper. A triangular pyramid with the bottom length of 82 mm and the height of 23 mm is the basic unit of the truss core panel; the thickness of the plate on design is 1 mm. As shown in Fig. 2, the two truss core panels are combined as the vertices of the triangular pyramids on the plates facing each other and the vertices on one plate and the flat surface on the other plate are spotwelded.

**2.2 Outline of the Simulation for the Multistage Press Forming.** The truss core panel shown in Fig. 1 is the target of our multistage press forming simulation. The number of the truss cores is  $6 \times 5$  array. On the forming simulation, we change the

Contributed by the Applied Mechanics Division of ASME for publication in the JOURNAL OF APPLIED MECHANICS. Manuscript received December 11, 2008; final manuscript received July 17, 2009; published online February 8, 2010. Assoc. Editor: Vikram Deshpande.

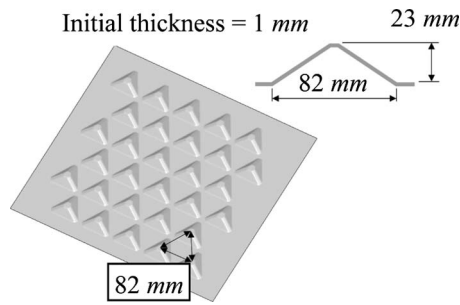


**Fig. 1 Typical geometry and dimensions of truss core panel**

shape of the truss core with geometrically complete triangular pyramid as follows, so as to be used and formed in practical member.

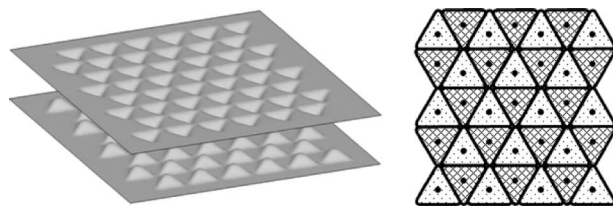
- (1) In order to spotweld at the vertex of the triangular pyramid, the vertex is made to a plateau.
- (2) The edges and bottom face of the triangular pyramid are both made round.

Figure 3 shows the analysis model used in the forming simulation. The model consists of a blank, die, punch, and holder. The authors adopted SPCE (Steel Plate Cold-formed deep drawn Extra, defined in Japanese Industrial Standards), steel plate for deep drawing, as the blank material because of well formability and inexpensiveness. The yield function is based on the yield function of Hill [6] in 1948. Applying the conditions for in-plane isotropy and plane stress state to the yield function and assuming the plastic strain rate obeys the associated flow rule, we can get the following equation as the yield function [7]

$$f(\sigma) = \left( \sigma_{11}^2 + \sigma_{22}^2 - \frac{2r}{r+1} \sigma_{11}\sigma_{22} + 2\frac{2r+1}{r+1} \sigma_{12}^2 \right)^{1/2} \quad (1)$$

this yield function is used in the simulation where  $\sigma_{ij}$  ( $i, j=1, 2$ ) is the component of the stress tensor and  $r$  is the Lankford's  $r$  constant. The material properties shown in Table 1 and Fig. 4 are used in the simulation. It is widely known that a larger  $r$  constant means higher formability. The blank material has the  $r$  constant of 1.815, which is a relatively large value. This is why the authors adopted SPCE as the blank material.

In forming of the truss core panel, the authors have shown the



**Fig. 2 Combination pattern of lower and upper truss core panels**

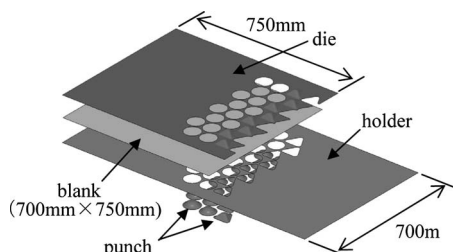


**Fig. 3 Multistage forming model**

**Table 1 Material properties (SPCE)**

Young's modulus	206 GPa
Poisson's ratio	0.3
Yield stress	159.74 MPa
Density	$7.84 \times 10^3$ kg/m <sup>3</sup>
$r$	1.815

difficulty in single stage forming because of the occurrence of cracks caused by large stretch around the vertex of the triangular pyramid in [4]. Then, a multistage forming procedure has been proposed by the authors. In this procedure, a region of blank for one truss core is formed first as a hemispherical shape with hemispherical punch in the preforming stage, and next, this region is formed into a triangular pyramid with pyramidlike punch. Employing this procedure, eight stages are necessary in order to form a truss core panel with the  $6 \times 5$  array. In the simulation, the blank is divided into quadrilateral shell elements with the edge length of 1.2 mm. The element type used in the blank is a four-noded reduced integration quadrilateral shell element with a viscous type hourglass control [8,9] and is widely used in explicit FEM software. One Gaussian integration point for in-plane and three-points for through-thickness integration are defined in each shell element. The die, the punch, and the holder are all defined as rigid.

Stress and strain distribution and thickness distribution obtained in each former stage are all transferred into the subsequent stages. Figure 5 shows the blank geometry obtained by the final result of multistage forming process.

**2.3 Procedure to Create the Three-Point Bending Analysis Model.** A model for bending analysis is constructed on the basis of the truss core panel model obtained by the above forming simulation. The build-up procedure is described as follows:

- (1) The size of the truss core panel after the forming is about  $727 \times 713$  mm<sup>2</sup> including the flange. The panel is trimmed to  $612 \times 655$  mm<sup>2</sup>. In the trimming, the elements on the trimline are divided along the trimline. Figure 6 shows the trimline and the truss core panel after the forming.
- (2) In order to obtain excessively accurate local distributions of stress, equivalent plastic strain, and thickness in the press forming simulation, element size of 1.2 mm quadrilateral shell elements is adopted, which is as almost the same as the initial thickness (1.0 mm) of the blank. On the other hand in the bending analysis, the elements with edge length of 5 mm are used to shorten the computation time. To trans-

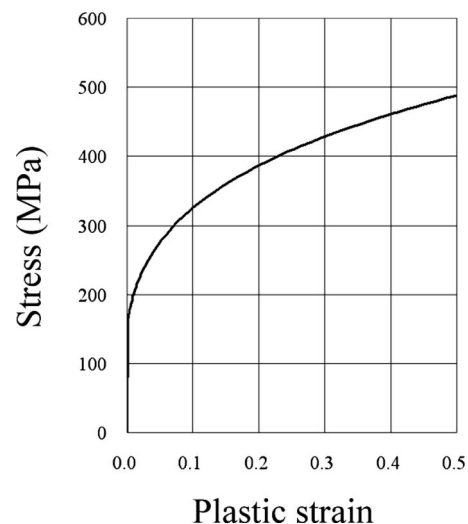


**Fig. 4 Stress-plastic strain curve (SPCE)**

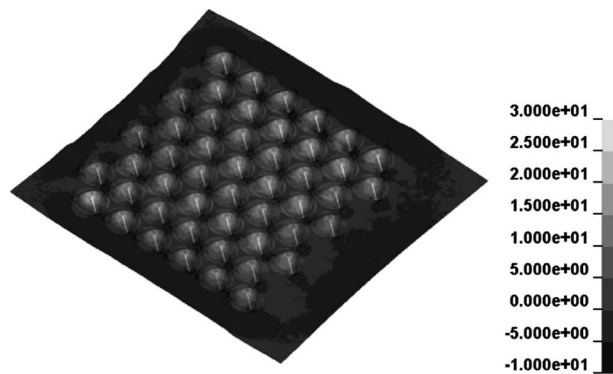


**Fig. 5 Final result of multistage forming process with thickness reduction (%)**

for stress/strain states and thickness from the fine mesh to the coarse mesh, a mapping procedure should be performed. Figure 7(a) shows the meshes used in the simulation of the press forming and the bending analysis. Since the reduced integration shell formulation is used through the simulation, stress, strain, and thickness values are updated and stored at only one integration point located at the center of each element. First in the mapping procedure, the nearest element in the fine mesh to the center of an element in the coarse mesh is searched. Second, the values (stress, strain, and thickness) of the nearest element are mapped to the integration point at the center of the element in the coarse mesh as shown in Fig. 7(b).

- (3) A truss core panel involving stress, equivalent plastic strain, and thickness is duplicated and turned around upside down. At the time, the stress tensors of the panel turned around are transformed according to the usual way to rotate second order tensor.
- (4) Several possible patterns can be considered to combine upward and downward truss core panels, e.g., attaching ridgelines of the pyramids and so on. However, a strict accuracy is required in the case of attaching ridgelines and real production cost may be more expensive. Then, in this paper, the combination pattern shown in Fig. 2 is employed because the production may be easier. Real truss core panels may be combined with spotwelds between the tops of the pyramids on one plate and flat area of the other one. So the modeling technique using beam element to represent a spotweld is adopted, which is commonly used in FE simulation. Figure 8 shows the conceptual diagram of the spotweld beam model. In this method, the nodes at the both ends of a beam element corresponding to a spotwelded points can be placed at an arbitrary position on the surface of shell element to be spotwelded. The degree of freedom

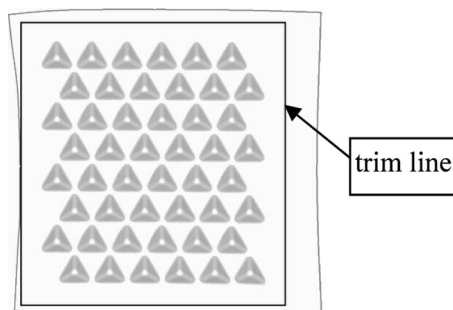
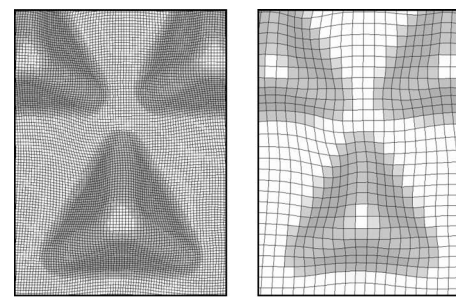
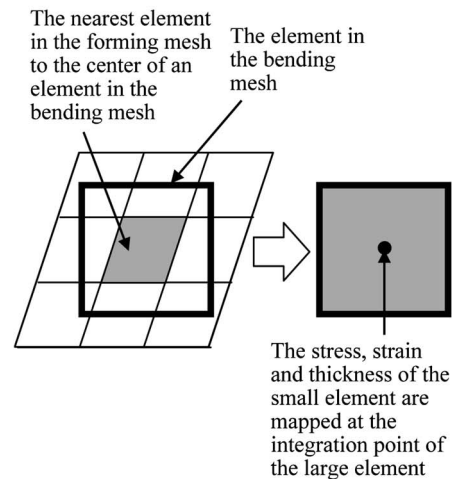


**Fig. 6 Final geometry of formed blank and trim line**



**(a) forming mesh (left) and bending mesh (right)**



**(b) Mapping of stress, strain and thickness**

**Fig. 7 Mesh density of forming mesh (1.2 mm) and bending mesh (5 mm) and mapping algorithm**

of spotweld nodes are constrained by the nodes composing shell element.

- (5) Two supports are set under the both ends of the welded truss core panels and a punch is set on the center of the panels. The supports and the punch are all rigid and the geometry of these tools is a cylinder with 100 mm diameter. Figure 9 shows the entire configuration of the model for the three-point bending analysis.

**2.4 Modeling of Honeycomb Panel and Verification.** In order to compare the bending stiffness of the truss core panel with honeycomb panel, FE model of honeycomb panel should be created. Before comparing truss core panel and honeycomb panel, an aluminum honeycomb panel, which has the result of actual three-point bending test was modeled the accuracy of the model was verified based on the test result. Figure 10 shows the dimensions

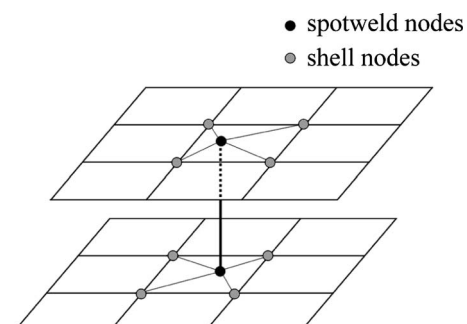


**Fig. 8 Definition of spotweld using beam element**



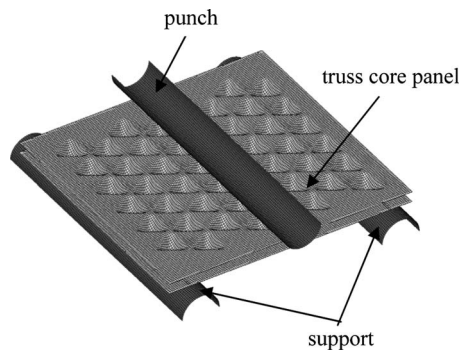


**Fig. 9 Truss core panel model configuration for bending analysis**

of the honeycomb model. Since the honeycomb cells are formed from glued two plates as shown in Fig. 10, the thickness of the shell elements in glued region is set to twice of the one in the nonglued region. The thickness of upper and lower surface plates sandwiching honeycomb cells are 1.0 mm and 0.5 mm, respectively. The material properties used in the simulation are Young's modulus of 70.4 GPa, Poisson's ratio of 0.33, and yield stress of 54.94 MPa. The stress ( $\sigma_y$ ) versus plastic strain ( $\epsilon_p$ ) curve beyond the yield point is approximated by Swift's formula in Eq. (2)

$$\sigma_y(\epsilon_p) = K(\epsilon_0 + \epsilon_p)^n, \quad \epsilon_0 = \left( \frac{\sigma_{y0}}{K} \right)^{1/n} \quad (2)$$

where the parameters  $K$  and  $n$  are 183.60 MPa and 0.125, respectively. The  $\sigma_{y0}$  in Eq. (2) is the initial yield stress. In addition, sudden decreasing for the bending strength caused by crack opening in the lower surface plate was observed in the experiment. So in the analysis, it is assumed that elements fail when the value of equivalent plastic strain of the elements reaches to 0.09 and the elements are eliminated from the calculation. The analysis conditions are defined following the test condition, i.e., the span between the supports is 275 mm and the enforced displacement on the centered punch is 20 mm. The members of the supports are completely fixed. In addition, the penalty based contact conditions are defined between the punch and the honeycomb panel and between the honeycomb panel and the supports, and self-contact condition is also defined for the honeycomb panel itself. Figure 11 shows the comparison of the results of the analysis and the experiment. Figure 11(a) shows the distribution of equivalent plastic strain on the honeycomb panel obtained from the analysis and the photograph of the experiment. The location of the failure (elimination of elements) by the analysis and of the crack by the experiment is quite similar. Figure 11(b) shows the comparison of the force-displacement (punch stroke) curves from the analysis and the experiment. The both curves show good correlation and the maximum strength and the reductions in strength caused by the failure in the lower surface plate are captured properly. The oscillation is seen in the graph from the analysis during force increasing and soon after the failure. The reason is why as the analysis does not consider damping mechanism such as structural damping

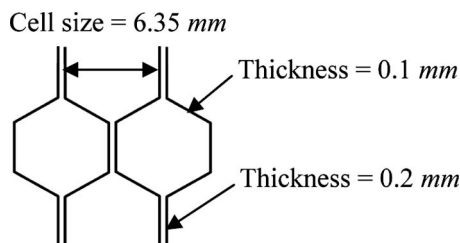
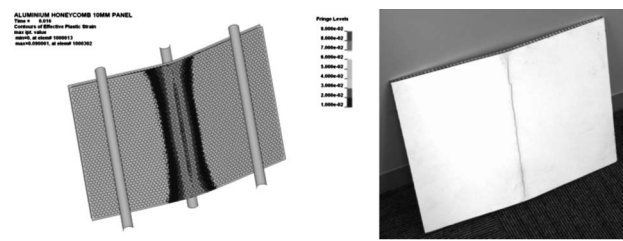
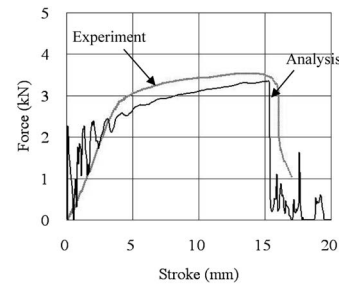


**Fig. 10 Honeycomb cell structure and dimensions**



**(a) Deformation and failure of honeycomb core panel**



**(b) Force-displacement curve**

**Fig. 11 Comparison of analysis and experiment**

and so on, it induces the numerical oscillation inherent in the dynamic analysis using explicit method. With these comparisons, it was shown that the FE model of the created honeycomb panel could reproduce the behavior for bending of the actual honeycomb panel. Based on this modeling technique, we also make a model of steel honeycomb panel below.

### 3 Analysis Condition

As the boundary conditions, the support members are completely fixed and enforced displacement is applied to the punch in the  $z$ -direction. Contact surfaces based on the penalty method are defined between the truss core panel and the punch and between the panel and the supports. A penalty based contact condition is also defined on the truss core panel assuming self-contact.

With or without considerations for the work hardening (stress and equivalent plastic strain distribution) of the truss core panel and thickness change caused by forming, and shell formulations give four analysis cases shown in Table 2. Two types of shell element formulation are employed as typical elements frequently used in explicit FEM, namely, the Bathe–Dvorkin full integration shell element [10] (four in-plane integration points) and the Belytschko–Tsay reduced integration shell element [8] (one in-plane integration point) where the number of the integration points for the through-thickness direction is three for the both formulations.

In order to compare bending stiffness, a honeycomb panel model is created again and bending analysis is performed under the same analysis conditions as the truss core panel. The dimensions of honeycomb are decided as follows; small regular hexa-

**Table 2 Analysis cases**

Case	Model	Work hardening	Thickness change	Shell formulation
1	Truss core	○	○	Full int.
2	Truss core	×	○	Full int.
3	Truss core	×	×	Full int.
4	Truss core	○	○	Reduced int.
5	Honeycomb	×	×	Full int.

○: included; ×: not included.

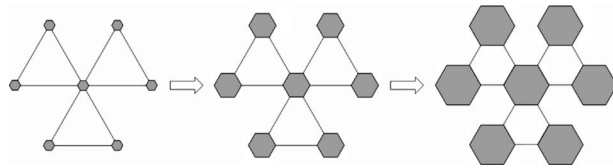


Fig. 12 Transformation of truss core to honeycomb

gons are inserted into the apexes of triangles of the truss core bottom, as shown in Fig. 12, and using an operation called truncation, honeycomb structure is built by enlarging the regular hexagons till the edge length of the regular hexagons becomes to 1/3 of the edge length of the triangle. As honeycomb is formed by bending only, we assume that the forming does not affect the thickness change and hardening of the material for honeycomb. The dimensions of both the honeycomb panel and the truss core panel are  $612 \times 655 \times 27.3 \text{ mm}^3$ . The thickness of the upper and lower surface plates and the wall thickness of the honeycomb core are all 1.0 mm. The mass of the created honeycomb is 9.154 kg and the one of the truss core panel is 6.935 kg. The relative density of honeycomb panel  $\bar{\rho}_h$  is defined as the mass of honeycomb panel divided by the mass of solid metal block with same dimensions. The relative density of truss core panel  $\bar{\rho}_t$  is also defined in the same way. The values of  $\bar{\rho}_h=0.1068$  and  $\bar{\rho}_t=0.0809$  are obtained with the density in Table 1. It is known that the strength (nominal stress-strain relation) of “core panel” structure for out-of-plane loading is related with relative density [11]. The peak stress and absorbed energy for the panels against collapse load are changed in accordance with relative density [12]. The comparison of mechanical response should be made between the honeycomb panel and the truss core panel with same relative densities. The current ratio of  $\bar{\rho}_h$  and  $\bar{\rho}_t$  is 1.32. Then the honeycomb will be considered more advantageous in comparing stiffness per unit mass than the truss core panel. In order to equalize the relative densities of both panels, the thickness of the honeycomb panel is thinned to 0.758 mm that means 1/1.32 of the initial thickness of 1.0 mm. Figure 13 shows the geometry of the honeycomb model.

#### 4 Results and Discussion

As an example for the bending analysis of truss core panel, the deformation of the panel of case 1 in Table 2 are shown in Fig. 14. For the other analysis cases, there is no obvious difference for the deformed geometry. By plotting the contact force between the punch and the panel versus the punch stroke, the bending stiffness of the two panels are compared. Figure 15 shows the contact force-punch stroke curves. The case in which both of work hardening and the thickness change are considered (case 1) shows the strength of 1.6 times higher than the case in which both of them are not considered (case 3). The results of the analyses show clearly that it is absolutely necessary to consider the effect of work hardening in case of estimating bending stiffness of truss

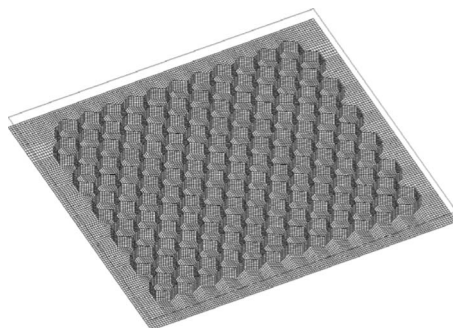


Fig. 13 Honeycomb model (upper plate invisible)

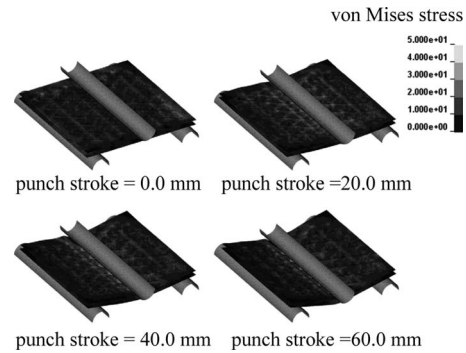


Fig. 14 Deformation and von Mises stress distribution on truss core panel

core panel formed from thin metal plate. Indeed, it should be verified whether the effect of work hardening is actually so large or not by bending experiment for real truss core panel processed in press forming. In addition, there is only a little difference between the case where only thickness change is considered (case 2) and another case where both of thickness change and work hardening are not considered (case 3).

In the comparison on the formulations of the shell element, the Belytschko–Tsay reduced integration shell element (case 4) shows about 22% lower strength in comparing with the Bathe–Dvorkin full integration shell element (case 1). Referring the description in Ref. [8], it is supposed that low bending stiffness of the Belytschko–Tsay shell element in this case comes from the formulation of this element based on the assumption that the element geometry is flat. It is known that the accuracy (stiffness) of this element is decreased as the warpage becomes over 5 deg. On the other hand, as the Bathe–Dvorkin full integration shell element reflects information of warping on each node, the accuracy is hardly reduced for nonflat, twisted element. The dark elements in Fig. 16 show the elements that their warpage exceeds 5 deg. In this model, the rate of the elements with warpage of over 5 deg for the ones of the whole model is 32%. As the model has many warped elements, the accuracy of the solution will be decreased in the case of using the Belytschko–Tsay reduced integration shell element. In the comparison of the bending stiffness for the truss core panel and the honeycomb panel, the bending stiffness of truss core panel considering work hardening (case 1) is about 80% of one of the honeycomb panel (case 5). However, there is a possibility of failure in the surface plate of the honeycomb panel, as

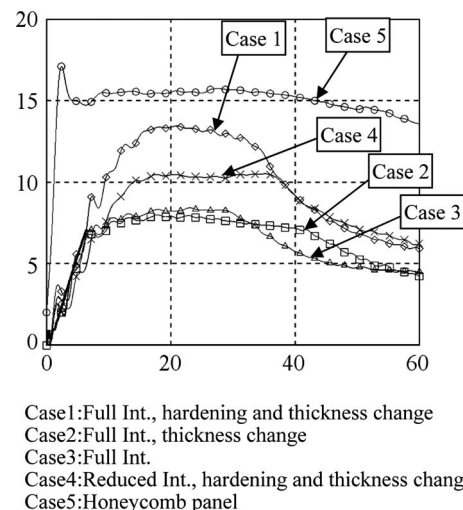
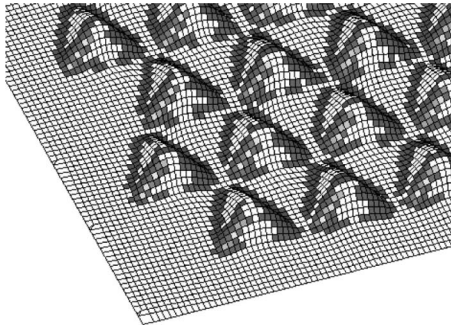


Fig. 15 Force-stroke curve



**Fig. 16 Dark elements have warpage of over 5 deg**

seen from the result of the bending simulation of honeycomb panel shown in Fig. 11. For SPCE, equivalent plastic strain of about 25% is generally used as the failure criteria. According to the analysis, the value of equivalent strain reaches to 25% at the displacement of the punch stroke to be about 30 mm. Therefore, the strength of the honeycomb panel in Fig. 15 may be decreased quickly as the punch stroke becomes over 30 mm if the failure criteria are considered in the simulation. From the point of view of energy absorption, truss core panel will have higher advantage than honeycomb panel in failed case. Even more, truss core panel will have sufficient availability by considering its flame resistance.

## 5 Conclusions

The procedure to create a practical truss core panel structure model using the formed geometry, six components of stress, equivalent plastic strain, and thickness distribution obtained from the multistage forming simulation was presented. And the three-point bending analyses considering work hardening effects using the developed model were performed. Also, we compared the bending stiffness for the cases with or without consideration of work hardening effect and the cases of two different shell formulations. From the results, the possibility that the effect of work hardening would dominate the bending stiffness of truss core panel was revealed. On the formulation of shell element, it was shown that high accuracy in bending analysis could not be obtained as long as shell element in which warpage was adequately reflected in the element stiffness was employed.

In addition, a finite element model of honeycomb panel was created and basic comparison for the bending stiffness of truss core panel and the honeycomb panel was performed.

In the future, quantitative verification of work hardening effect should be made through experiment. For the comparison of strength between the truss core panel and the honeycomb panel, more detailed modeling of honeycomb panel considering failure of honeycomb and tearing on the glued surface is necessary to investigate more realistic bending stiffness through the simulation. It will also be necessary to compare strengths of truss core panel and honeycomb panel for different loadings such as shearing, compression and so on, adding to bending.

## Acknowledgment

The CAD data of the truss core panels and the photographs of trial products used in the research work were delivered by Mr. You Gotou and Mr. Haruo Suzuki at Shiroyama Industry Co., Ltd. Several parts of the research work were carried out by the support of the institution of the basic research promotion in transportation field by the independent administrative institution, Japan Railway Construction, Transport and Technology Agency and Grants-in-Aid for scientific research (category S) under Grant No. 20226006. We acknowledge their aids dearly.

## References

- [1] Nojima, T., and Saito, K., 2007, "Panel and Panel Production Method," Japanese Patent Disclosure No. 2007-023661.
- [2] Nojima, T., 2007, "Panel and Panel Pieces," Japanese Patent Disclosure No. 2007-055143.
- [3] Saito, K., and Nojima, T., 2007, "Modeling of New Light-Weight, Rigid Core Panels Based on Geometric Plane Tilings and Space Fillings," *Trans. Jpn. Soc. Mech. Eng., Ser. A*, **73**(735), pp. 102–108.
- [4] Tokura, S., and Hagiwara, I., 2008, "Forming Process Simulation of Truss Core Panel," *Trans. Jpn. Soc. Mech. Eng., Ser. A*, **74**(746), pp. 1379–1385.
- [5] Hallquist, J. O., 2007, *LS-DYNA Keyword User's Manual*, LSTC.
- [6] Hill, R., 1948, "A Theory of the Yielding and Plastic Flow of Anisotropic Metals," *Proc. R. Soc. London, Ser. A, Math. and Phys. Sci.*, **193**(1033), pp. 281–297.
- [7] Hallquist, J. O., 2007, *LS-DYNA Keyword User's Manual*, LSTC, pp. 171–174.
- [8] Belytschko, T., and Tsay, C. S., 1984, "Explicit Algorithms for Nonlinear Dynamics of Shells," *Comput. Methods Appl. Mech. Eng.*, **43**, pp. 251–276.
- [9] Belytschko, T., and Tsay, C. S., 1983, "A Stabilization Procedure for the Quadrilateral Plate Element With One-Point Quadrature," *Int. J. Numer. Methods Eng.*, **19**, pp. 405–419.
- [10] Bathe, K. J., and Dvorkin, E. D., 1985, "Short Communication a Four-Node Plate Bending Element Based on Mindlin/Reissner Plate Theory and a Mixed Interpolation," *Int. J. Numer. Methods Eng.*, **21**, pp. 367–383.
- [11] Zupan, M., Chen, C., and Fleck, N. A., 2003, "The Plastic Collapse and Energy Absorption Capacity of Egg-Box Panels," *Int. J. Mech. Sci.*, **45**, pp. 851–871.
- [12] Akisanya, A. R., and Fleck, N. A., 2006, "Plastic Collapse of Thin-Walled Frusta and Egg-Box Material Under Shear and Normal Loading," *Int. J. Mech. Sci.*, **48**, pp. 799–808.